Building An Electron Spectrometer: Characterizing Electron Beam for FLASH Radiotherapy
REU Program at Columbia University - Nevis Labs, Radiological Research Accelerator Facility

Alana Ho[1]

[1]Wellesley College, Wellesley, MA

August 1, 2025

Abstract

FLASH radiotherapy (RT) is a technique that uses ultra-high dose rate irradiation (>40 Gy/s) to target tumors while reducing radiation effects on surrounding healthy tissue. FLASH RT is an experimental Ultra-High Dose Rate (UHDR) method of RT. The aim of this paper is to characterize the energy of the electron beam using a modified Varian Clinac 2100C. The device was prototyped and built using 2 neodymium magnets, a 1 mm lead aperture to focus the beam, GAFChromatic EBT3 film sheets, and a 3D printed mount. This project was approached with the engineering design process to optimize data collection and discover changes that could be made.

Contents

1 Introduction

Radiotherapy (RT) is a commonly implemented treatment for cancer. Often, radiotherapy treatment uses a high-energy beam. External beam radiation targets cancer cells by causing cellular damage more rapidly than the cell's ability to self-repair [1]. Using a linear accelerator, radiation is delivered with either X-rays or electron beams.

Conventional radiotherapy uses Bremsstrahlung X-rays created by stopping electrons on a tungsten target. These irradiations are focused on the tumor area; however, adjacent normal tissue cells are damaged to a similar degree, causing disease, pain, or mutation. To combat this, lower doses are administered in a series of radiation sessions. This is called fractionation, a process in which daily sub-lethal doses (2 Gy/fraction) are delivered over a few weeks [2]. An alternative modality of RT is FLASH. FLASH radiotherapy is a technique that uses ultra-high dose rate irradiation (>40 Gy/s) to target tumors while reducing radiation effects on normal tissue[3]. This is a promising, yet bio-mechanically less understood method of providing the necessary dose while limiting radiation to surrounding healthy tissue. The Radiological Research Accelerator Facility (RARAF) at Columbia University's Nevis Laboratories uses an electron beam to deliver radiation and study FLASH radiotherapy.

1.1 FLASH Therapy

Conventional radiotherapy is limited by its adverse effects on surrounding healthy tissue. Past procedures that lacked incremental treatments had greater adverse effects than successes. However, in the 1920s, periodic treatments at lower dose rates were discovered to prevent severe side effects [1].

Despite discoveries on fractionated treatment, normal tissue toxicity continues to be a drawback for radiation therapy. FLASH therapy is an experimental Ultra-High Dose Rate (UHDR) method of RT. Even though FLASH RT has an average dose rate of 40 Gy/s, the equivalent dose is equal to conventional RT.

FLASH RT is still in its preclinical testing stages, but it has shown promise in irradiating cancerous tissue and sparing other tissue[4]. This phenomenon is likely due to hypoxia-induced radio-resistance —tumors naturally have low oxygen, whereas normal tissue is more oxygenated [5]. Yet, this phenomenon is only observed experimentally at doses below 30 Gy in organs including the lungs and brain [6].

1.2 Characterizing the Electron Beam

One step towards improving the understanding of FLASH RT is by characterizing the energy of the electron beam. This is important information for accurately measuring and analyzing the beam properties and their effects, in addition to ensuring consistent results. This project characterizes the electron beam by building an electron spectrometer and measuring the deflection of the beam using GAFChromic EBT3 film.

2 Methods

2.1 Modified Clinical Linear Accelerator

Linear accelerators used for medical irradiation are small-scale accelerators. They are the main devices used for radiotherapy. A clinical linear accelerator is a linear particle accelerator that can operate at multiple energy levels: 6 MeV, 9 MeV, 12 MeV, 16 MeV, and 20 MeV. Each energy penetrates at a different depth; the higher energy beams deposit radiation deeper into a

sample. The RARAF modified Varian Clinac 2100C operates in service mode with the options of firing an electron and photon beam. This decommissioned Clinac has a fixed gantry and a beam permanently pointing vertically up.

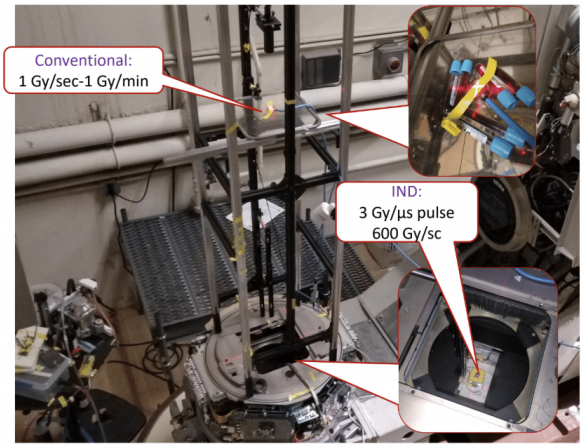

Figure 1: *RARAF modified Varian Clinac 2100C. Picture taken above the beam exit. Pictured are the optical rails and a platform where the electron spectrometer rested.*

In order to power the Clinac, microwave power is used to accelerate electrons from an electron gun along the length of the accelerator. They are then focused witha solenoid magnet and bent through a 270-degree magnetic dipole. To begin this process, a radiofrequency (RF) driver generates the microwaves, which are then amplified by a klystron. In an electron accelerator, two forms of radiation can be produced. With a target in place, electrons are converted into photons through the Bremsstrahlung process. Commissioned clinical linear accelerators use this method to produce X-rays because of their high penetration. Alternatively, when the target is removed, there is simply electron radiation. This is the radiation delivered at RARAF.

Due to the beam's conical shape, the spot size and dose rate can be adjusted by increasing or decreasing the distance from the beam exit. To make use of this, the clinac was fitted with optical rails and an experimental platform (Fig. 1). The platform can be raised or lowered, increasing or decreasing the distance from the beam exit. Another modification that can be made to the experiment is adjusting the size of the beam received. this is achieved using 1/4 inch lead or 1/2 inch copper shielding. The beam size for this project was reduced to a 1 mm diameter circle using a lead aperture.

2.2 Film Dosimetry

To accurately measure the radiation dose, GAFChromic EBT3 film is used (Fig. 2a) . This film works similarly to photographic film. After experiencing radiation, the film darkens in color and opacity [7]. The opacity is measured using a film scanner, converting opacity to dose. The film is scanned 1 to 2 hours after irradiation to allow for it to develop. The film is measured at 300 DPI, and the dose is calculated with the following equations:

$OpticalDensity = log10(PixelValueIrradiated/PixelValueControl))$

$Dose = (0.7404OpticalDensity/0.818OpticalDensity)$

These values are determined experimentally based on a control, non-irradiated section of the film from the same sheet. Each scan involves a control to compensate for potential variation in the scanner bulb intensity.

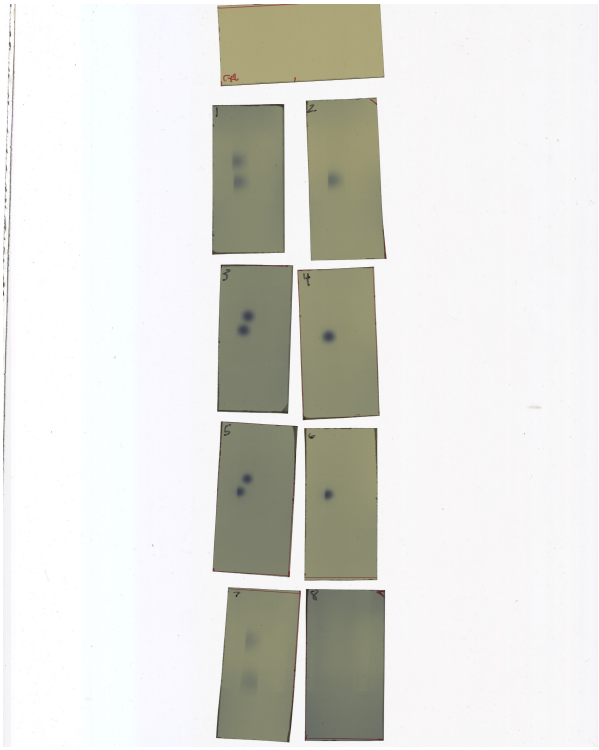

a) Scanned films.

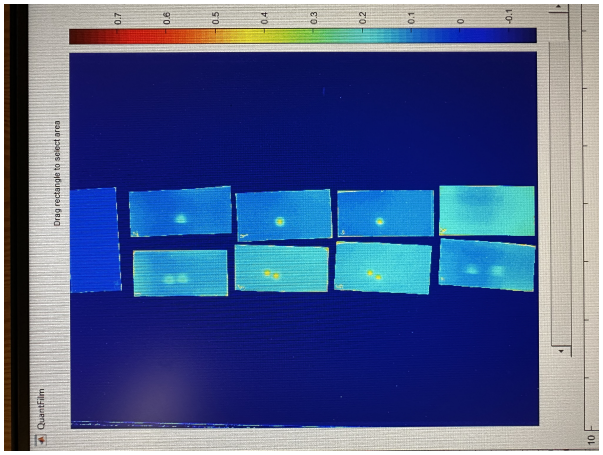

b) Processed films using dose MATLAB script.

Figure 2: *GAFChromic EBT3 films after irradiation with a 1 mm circular collimator aperture.*

Scanned films are processed using a MATLAB script. The .dat files are uploaded to the system, and the script recreates a cross-section of the film by scanning for maximum and average areas (Fig. 2b). To the left of the upload, a color gradient visualizes the dose. The control blends into the blue background by measuring a new calibration curve for each batch. Using a line tool to highlight a strip of film, each film can be plotted in a dose versus pixel graph. To improve the plots, the data can be averaged over several pixels, revealing peaks and removing noise.

2.3 Building an Electron Spectrometer

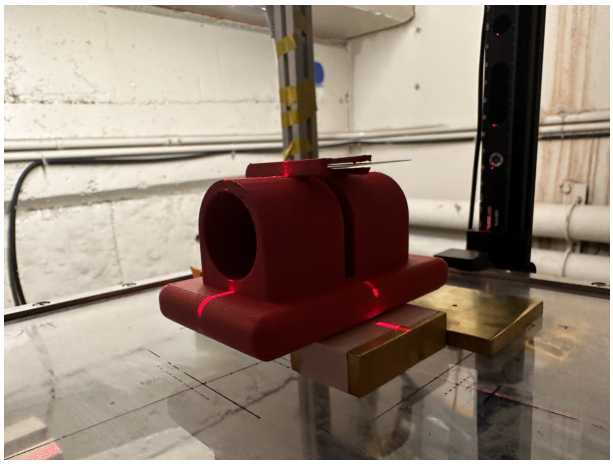

Figure 3: *Final Iteration of the Electron Spectrometer*

An electron spectrometer is an instrument used to measure the energy of an electron. For this build, magnets were used to measure the deflection of the electron in the magnetic field on a sheet of GAFChromic EBT3 film, and sequentially calculate the energy, in addition to the dose.

This build was approached with knowledge of the Lorentz force. Depending on the strength of the magnetic field, the charge of the particle, and its velocity, the particle will exhibit cyclotron motion. The radius can be calculated using the length of the field and the deflection. Once the radius is known, it can be plugged into the momentum equation, and then the relativistic energy equation, refer to Sec. 3.1.

To build this film, magnet, and lead aperture mount, this project was approached with the engineering design process. Once brainstorming was complete, a design was drawn and 3D modeled to be 3D printed. Each design's goal was to function as a mount in addition to using minimal filament and remaining simple. These designs were tested and evaluated to optimize data collection and identify potential improvements.

The first iteration of this device used a horseshoe-shaped magnet. The poles of this magnet were 1 inch apart with a measured field strength of 105 mT. A mount was 3D printed to hook onto the magnet (Fig. 4a) while also keeping the film in a constant position. An issue arose with the alignment of the lead aperture, so the design was improved to include a hold for it (Fig. 4b). For each energy level, the beam was fired at the film with and without the magnet in place. Once complete, the films were scanned and uploaded to a MATLAB script that was used to measure the deflection in pixels (Sec. 2.4). Although there was a visible deflection, it was too minimal to reliably characterize the energy of the beam. This iteration was proof of concept.

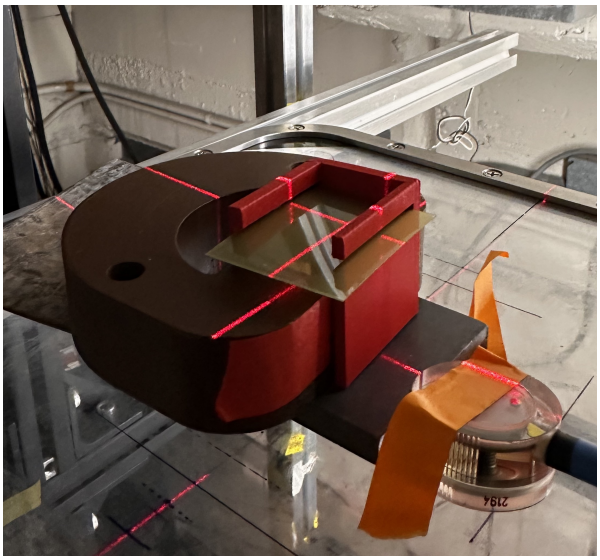

a) Mount fitted to magnet.

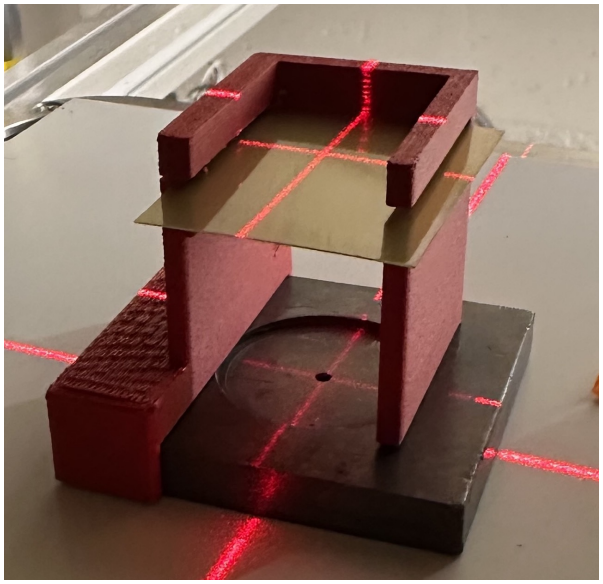

b) Mount with additional hold for lead aperture.

Figure 4: *The first iteration of the Electron Spectrometer using a horseshoe-shaped magnet*

To increase the deflection, a set of magnets with a surface field strength of 661.9 mT was tested. These magnets were cylindrical with a 1-inch diameter and a field perpendicular to the circular face. The first design kept the separation of the previous iteration, 1 inch apart, with a 200 mT field strength at the midpoint between the two magnets. The geometry was modified to hold the cylindrical magnets and the lead aperture (Fig. 5). After irradiating and scanning the film, the deflections measured were inconclusive. The mount was lowered from 170 cm to 100 cm above the beam exit to possibly increase the beam flux and the deflection, but there were only slight changes.

The final iteration of this mount decreased the distance between the magnets to 5 mm, and the measured field strength was 570 mT, much closer to the surface strength (Fig. 6). This change yielded a greater and measurable deflection. Additionally, to create a clearer scan and reduce noise, 1/4 inch lead and copper plates were placed around the mount (Fig. 3).

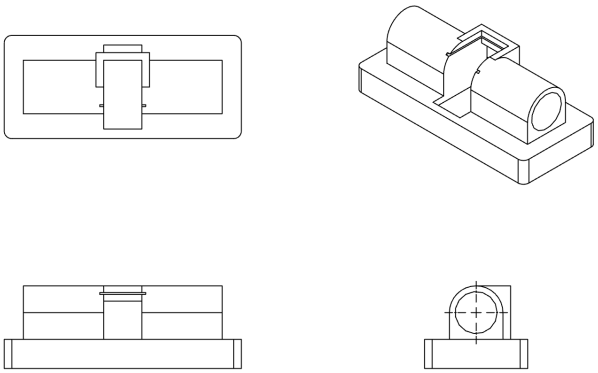

Figure 5: *Drawing of the Electron Spectrometer mount*

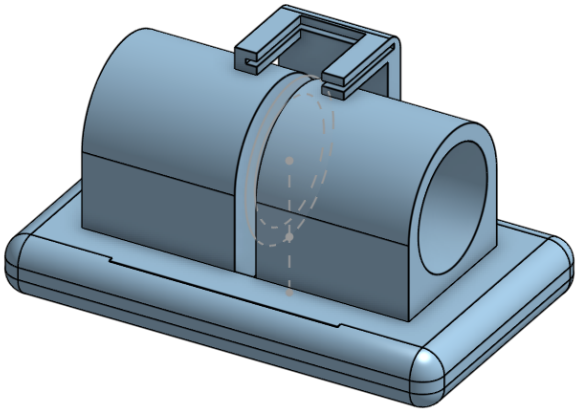

a) The Final 3D model of the Electron Spectrometer mount.

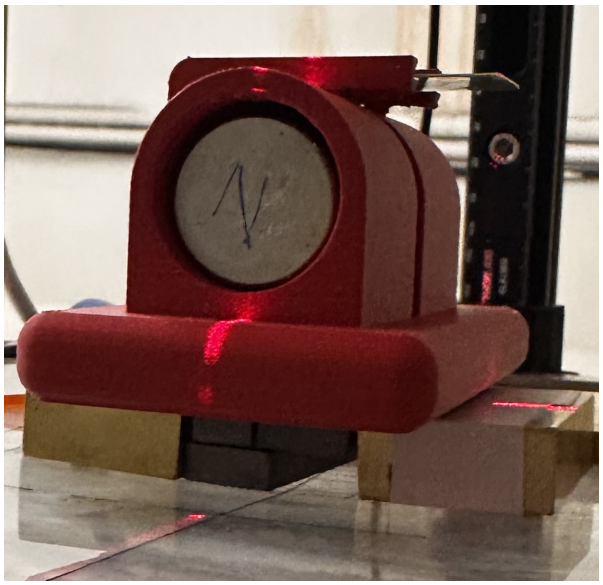

b) The Electron Spectrometer with copper and lead shielding.

Figure 6: *The final iteration of the Electron Spectrometer.*

2.4 Measuring Deflection

Using another MATLAB script, the .dat files are uploaded to Image Viewer, an image processing and computer vision app. To optimize this process and keep the film in a constant position within the mount, two films were used per energy level. The first measured the beam with and without the magnets in place. The second was layered on top of the first film to exclusively measure the deflected beam. The measure distance tool counts the pixels between a manually drawn line between the center of the two beam points. The diameter of each is also measured and used to calculate error.

Figure 7: *Film 1 from Trial 2 after processing with MATLAB Image Viewer script.*

3 Data, Analysis, and Results

3.1 Calculating the Energy of the Electron Beam

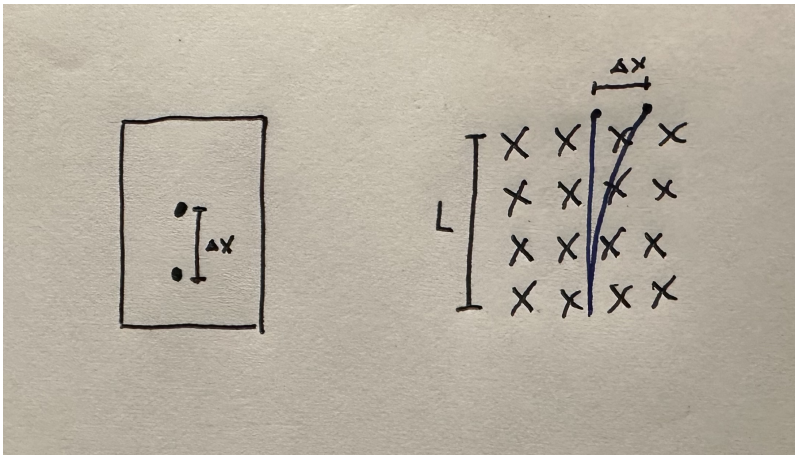

Figure 8: *Visualization of the deflection (x) from the perspective of the film (left) and the deflection from a cross section of the magnetic field (right). The length of the field (L) is based on the vertical path of the beam.*

After measuring the beam deflection, calculating the energy is as follows: $E = \sqrt{(pc^2) + (mc^2)^2}$ The constants and variables used are momentum (p), speed of light (c), the mass of an electron (m), the length of the field (L), the charge of an electron (q), magnetic field (B), and deflection (x). Refer to Fig. 8 for a visualization of the definition of the deflection and length of the field.

In order to use the relativistic energy equation, the deflection (x) is manipulated into radius ($r = L^2/2x$) and then plugged into the momentum equation ($p = qBr$).

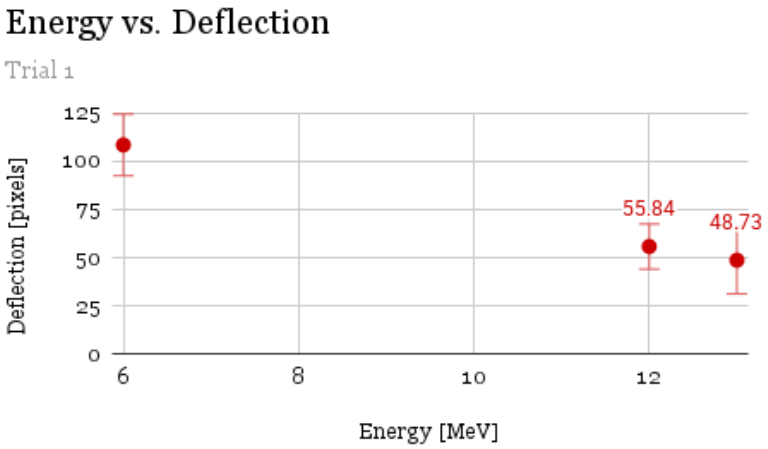

Figure 9: *Visualization of Trial 1 data.*

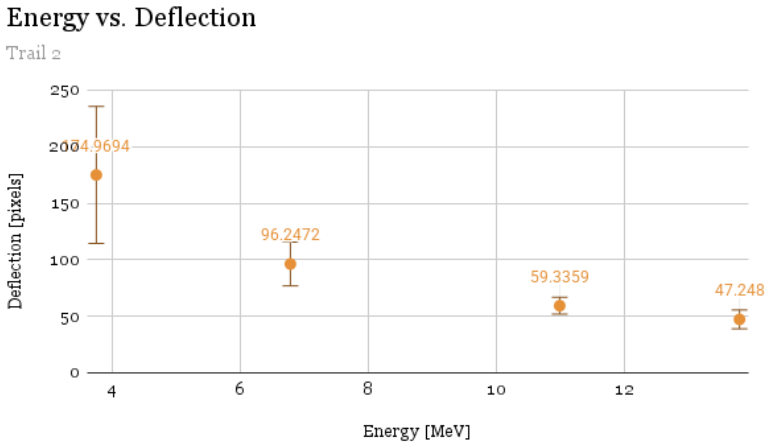

Figure 10: *Visualization of Trial 2 data.*

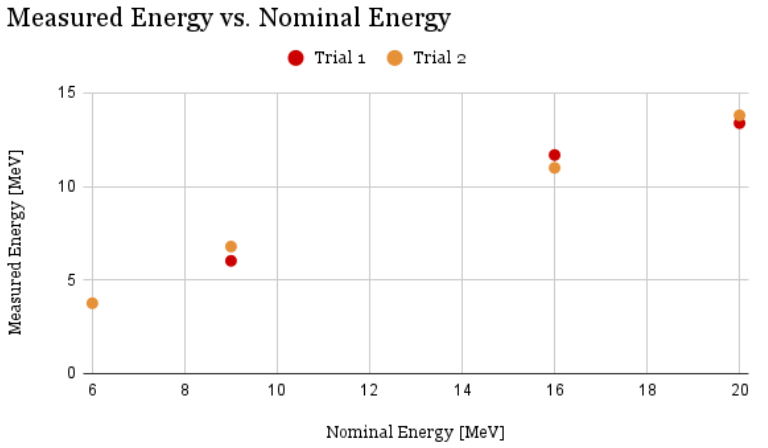

Figure 11: *Visualization of the measured energy compared to the assumed energy fired*

The calculated energy is then plotted against the deflection to understand their relationship as seen in Fig. 9 and 10. The error bars are derived from the radii of the marks on the film. In Fig. 11 , the measured and nominal energy are plotted against one another. The nonlinearity

highlights the difference in the measured and nominal energy. This data reveals that the energy that is assumed to be fired is not the same as the energy received. This is important information to acknowledge because knowing the actual energy being delivered, rather than just the nominal value, is crucial for accurately interpreting experimental results and understanding the system's behavior. Without this awareness, any analysis based on assumed values may lead to incorrect conclusions about the underlying physics.

3.2 Measuring Dose

Using the data collected from the film dosimetry MATLAB script, described in Sec. 2.2 , the dose can be used to cross-check the beam intensity with the deflection accuracy. This is achieved using dose data collected during experimentation from a NIST-traceable ionization chamber or a dosimeter. During experimentation, the dose was recorded after each film's irradiation period. They each received approximately 10 Gy, except for the 20 MeV beam in Trial 2, where the film was rendered unreadable due to excessive background. The dose was measured using a dosimeter placed next to the electron spectrometer. The dosimeter measures dose over 1 cm, but the film receives dose through a 1 mm aperture; therefore, the dose recorded (10 Gy) is less than that of the actual dose. Referencing the recorded dose (10 Gy) and comparing it to the dose based on the film dosimetry in Fig. 12 , the calculated energies are verified because the figures reflect the expected doses.

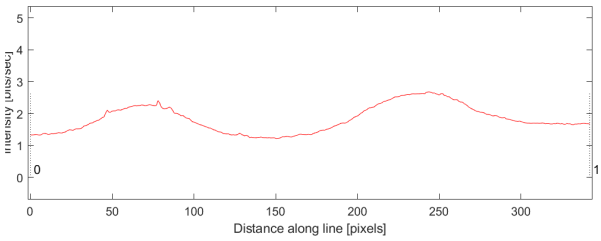

a) 6 MeV Intensity vs Pixel graph.

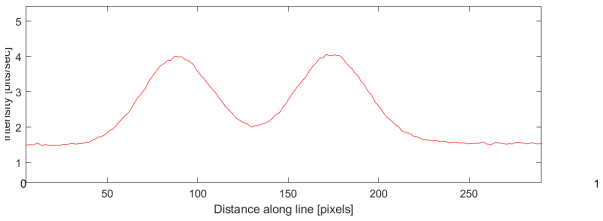

b) 9 MeV Intensity vs Pixel graph.

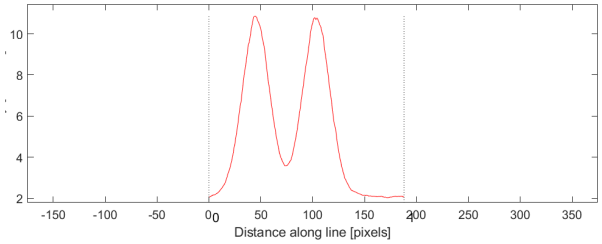

c) 16 MeV Intensity vs Pixel graph.

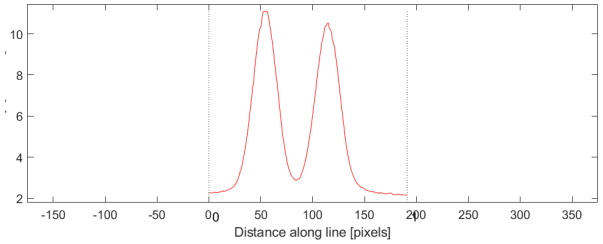

d) 20 MeV Intensity vs Pixel graph.

Figure 12: *Graphs of the Intensity vs Pixel for each energy level. Using the same film, the beam was fired without and with the magnets in place to optimize the process of measuring the deflection. This resulted in two peaks when scanned. The intensity (bits/sec) is converted to dose.*

4 Summary and Conclusions

4.1 Summary

FLASH RT is a strong candidate in the advancement of radiation technology. Providing ultra-high dose rates, it has proven to be a successful method of killing tumors while sparing healthy tissue [8]. The Radiological Research Accelerator Facility experiments with FLASH RT using a modified Varian Clinac 2100C to prepare for pre-clinical testing. In order to best understand the effects of FLASH, the electron beam used at different energy levels must be characterized.

The characterization of the electron beam is completed using an electron spectrometer. This device was prototyped and built using 2 neodymium magnets, a 1 mm lead aperture to focus the beam, EBT3 film sheets, and a 3D printed mount. With an understanding of the energies emitted, the usage of FLASH RT can be optimized.

4.2 Future Studies

This project is the foundation for future studies with a degraded beam. Using a similar methodology, a low-energy degraded beam can be characterized by measuring the deflection and calculating the energy. This process is more complex because it involves a slab of solid water plastic. The solid water scatters the beam, so collimating it for deflection measurement is difficult. Thus far, this challenge has been approached first using a 1 mm aperture placed directly on top of the slab. The film was illegible because the large beam scattering resulted in background from around the aperture.

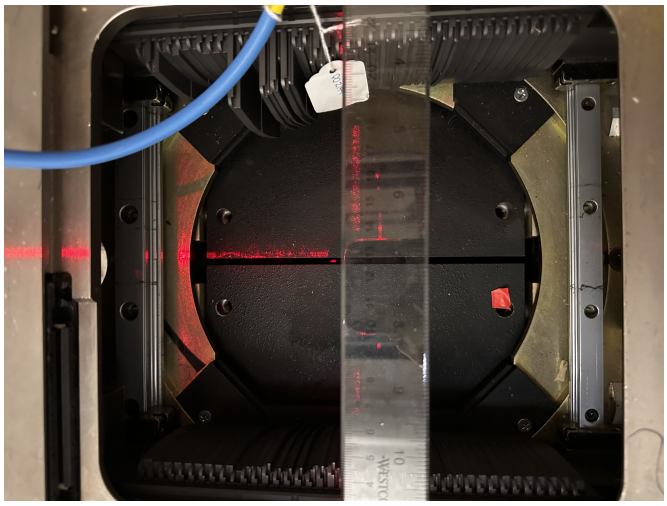

Figure 13: *Birds-eye view of the jaws of the clinac closed to provide a thin beam and shielding.*

To combat this, shielding jaws on the clinac were closed (Fig. 13) with the solid water slab sandwiched between two 1 mm collimators. Because the collimators and jaw opening were difficult to align, a mount was 3D printed (Fig. 14). This study will determine the energy of a degraded beam so that it can be accurately recorded and used to understand RT at low energy.

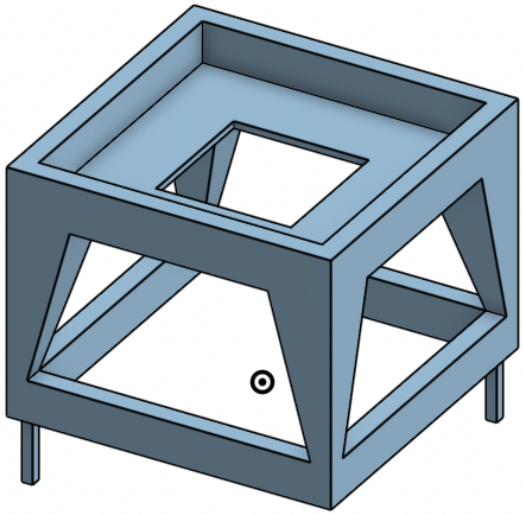

Figure 14: *CAD model of the aligning mount.*

5 Acknowledgments

This material is based upon work supported by the National Science Foundation under Grant No. PHY-2349438. Thank you, NSF, for this research opportunity! Additionally, thank you, Nevis Labs, for providing this research and engineering project, specifically Dr. Guy Garty, for his mentorship and support throughout this summer program. Dr. Yuewen Tan, Naresh Deoli, and Andrew Harken were an amazing team to work with at RARAF. Thank you for your constant assistance and education during daily experiments. This work was partially supported by grant number U19-AI067773 from the National Institute of Allergy and Infectious Diseases (NIAID), National Institutes of Health (NIH). The Clinac at RARAF was a gift from Weill Cornell Medicine, initiated by Dr. Silvia Formenti, with additional support from the Radiation Oncology departments at Weill Cornell Medicine and Columbia University Irving Medical Center (Dr. Lisa Kachnic), as well as an unrestricted research gift from Mr. Barry Neustein

References

[1] S. Gianfaldoni *et al.*, "An overview on radiotherapy: From its history to its current applications in dermatology," *Open Access Maced. J. Med. Sci.*, 2017.

[2] K. K. Likharev, "Relativistic Particles in Electric and Magnetic Fields," *Essential Graduate Physics – Classical Electrodynamics*, LibreTexts. [Online]. Available: https://phys.libretexts.org/Bookshelves/Electricity_and_Magnetism/Essential_Graduate_Physics_-_Classical_Electrodynamics_(Likharev)/09%3A_Special_Relativity/9.06%3A_Relativistic_Particles_in_Electric_and_Magnetic_Fields

[3] G. Garty, R. Obaid, N. Deoli, E. Royba, Y. Tan, A. D. Harken, and D. J. Brenner, "Ultra-high dose rate FLASH irradiator at the radiological research accelerator facility," *Sci. Rep.*, vol. 12, no. 1, pp. 1–14, 2022.

[4] S. Y. Kalbasi and M. B. Devasia, "Clinical applications of FLASH radiotherapy," *Radiat. Oncol.*, vol. 29, no. 1, 2024. [Online]. Available: https://pmc.ncbi.nlm.nih.gov/articles/PMC10766858/

[5] M. S. Smyth *et al.*, "Current perspectives on ultra-high dose rate radiation," *Cancer Treat. Rev.*, vol. 82, 2019. [Online]. Available: https://pmc.ncbi.nlm.nih.gov/articles/PMC6850216/

[6] M.-C. Vozenin *et al.*, "Towards clinical translation of FLASH radiotherapy," *Clin. Oncol.*, 2022.

[7] M. A. Devic, "Comprehensive evaluation and new recommendations in the use of Gafchromic EBT3 film," *PLoS One*. [Online]. Available: https://pmc.ncbi.nlm.nih.gov/articles/PMC10766858/

[8] J. M. Favaudon *et al.*, "Ultrahigh dose-rate FLASH irradiation increases the differential response between normal and tumor tissue in mice," *Sci. Transl. Med.*, vol. 6, no. 245, 2014. [Online]. Available: https://pubmed.ncbi.nlm.nih.gov/31303340/. [Accessed: Jul. 22, 2025].